JOURNAL OF MATERIALS SCIENCE **37** (2002) 3641 – 3650

Processing sodium tellurite melts in low gravity drop shaft

Part II *Melt solidification and glass formation*

DONGMEI ZHU
Ceramic Engineering Department and Graduate Center for Materials Research, University of Missouri-Rolla, Rolla, MO 65409, USA
State Key Laboratory of Solidification Processing, Northwestern Polytechnical University, Xi'an, Shaanxi 710072, People's Republic of China
E-mail: dzhu@umr.edu

C. S. RAY
Ceramic Engineering Department and Graduate Center for Materials Research, University of Missouri-Rolla, Rolla, MO 65409, USA

M. MAKIHARA
Department of Optical Materials, Osaka National Research Institute, 1-8-31 Midorogaoka, Ikeda, Osaka 563-8577, Japan

WANCHENG ZHOU
State Key Laboratory of Solidification Processing, Northwestern Polytechnical University, Xi'an, Shaanxi 710072, People's Republic of China

D. E. DAY
Ceramic Engineering Department and Graduate Center for Materials Research, University of Missouri-Rolla, Rolla, MO 65409, USA

The effect of gravity on glass formation and crystallization of the $Na_2O \cdot 8TeO_2$ (NT_8) and $Na_2O \cdot 4TeO_2$ (NT_4) melts were investigated using the low gravity drop shaft at the Japan Microgravity Center (JAMIC). This drop shaft produces a low gravity of $<10^{-3}$ g for $\sim$10 s during free-fall and about 8 to 10 g for $\sim$5 s during deceleration of the capsule. The glass initially adhered to a small platinum heating coil was re-melted in low gravity. The melt detached from the heating coil during the high-g period and solidified after being splattered on a plate (substrate) located $\sim$4 cm below the heating coil. The parameters that were varied for the drop shaft experiments were the melt temperature and the substrate material on which the melt splattered. Like what was observed at 1-g (ground), the NT_8 splatters from the drop shaft experiments always formed glass, being independent of the melt temperature and the substrate material used. The splatters from the NT_4 melts partially crystallized in all the drop shaft experiments, even though this melt is an excellent glass former at 1-g. The splatter on a substrate of higher cooling ability such as copper had a smaller amount of crystals than the splatter on a substrate of smaller cooling ability such as glass or alumina. The glass transition temperature, heat capacity in the glass transition region, activation energy for crystallization and the infrared (IR) spectra for the drop shaft splatters were not significantly different from those for the similar splatters prepared at 1-g. However, the crystallization temperature of all the drop shaft splatters was 5 to 10°C lower than that of their 1-g counterparts. This result suggests that the NT_8 and NT_4 melts solidified under drop shaft conditions are less resistant to crystallization than the similar melts solidified at 1-g.

1. Introduction

The drastic reduction in hydrostatic pressure, sedimentation, buoyancy or gravity-driven convective flows in a low gravity environment have consequences on virtually all processes involving fluids such as the solidification of melts [1–3]. Since glasses also are traditionally prepared by solidifying melts, a variation in gravity level could affect the glass formation process(s) and, consequently, the properties of glasses. Gravity-driven convection, which is the primary cause for mixing and homogenization in fluid melts at 1-g, is ideally absent or highly suppressed in low gravity. Fluid flows caused

by diffusion and surface tension (Marangoni flow) also promote melt mixing, but these forces are several orders of magnitude weaker than the gravity-driven convection. So, it is logical to think that the melts processed in low gravity might be less chemically homogeneous and, thus, less resistant to crystallization than similar melts on earth. However, the observed results are just the opposite.

Results from numerous experiments [4–11] conducted to-date report that the glass forming tendency for a melt is enhanced by a factor of, at least, 3 to 4 in low gravity, and the glasses are more chemically homogeneous and more resistant to crystallization than identical glasses prepared on earth, although one exception [12] is also noted. In other words, the glass formation tendency, chemical homogeneity, and resistance to crystallization for a melt decrease with increasing gravity. These interesting results have considerable scientific and practical importance, and suggest that the low gravity environment may be advantageous for developing new glasses and glass-ceramics of improved quality that are difficult to prepare on earth.

The present work had several objectives such as understanding the phenomena for melt evaporation and the formation of solid particles from vapor in low gravity, and gaining further insight for the effect of gravity on glass formation and crystallization for glass forming melts. The drop shaft at the Japan Microgravity Center (JAMIC), which is presently the worlds' largest and produces a low gravity of $<10^{-3}$ g for ~10 s during free-fall and a high gravity of 8 to 10-g for ~5 s during deceleration of the capsule, was used for the experiments. Two compositions, $Na_2O \cdot 8TeO_2$ and $Na_2O \cdot 4TeO_2$ (hereafter referred to as NT_8 and NT_4, respectively) in the sodium-tellurite system were used. Both NT_8 and NT_4 compositions melt at a relatively low temperature (~475°C) forming highly fluid (like water) melts which are excellent glass former at 1-g (earth). A low melting temperature combined with a low viscosity at the melting temperature make these melts highly suitable for processing within the short low gravity duration (~10 s) available in the drop shaft.

The experiments and results for melt evaporation and formation of solid particles from the vapor of NT_8 and NT_4 melts in low gravity are reported [13] in part I of this paper. The results on the analysis and characterization of the melts remaining after evaporation and solidified under the drop shaft conditions are described in this part. The melt, which was held in a small platinum heating coil during evaporation in low gravity, see the following section for experimental procedure and also ref. [13], detached from the coil in high gravity (capsule deceleration) and solidified after being splattered on a plate located just below the coil. Thus, it is believed that these NT_8 and NT_4 melts in the present drop shaft experiments were solidified essentially at 8 to 10-g.

2. Experimental procedure

The experimental procedure and parameters, and the composition and preparation of the sodium tellurite glasses (NT_8 and NT_4) used in the present work are described in part I [13] of this paper. A description of the experimental apparatus and the drop shaft at JAMIC is also given in ref. [13]. The experimental apparatus basically consisted of a glass box (~5.0 cm × 5.0 cm × 7.6 cm) made with standard microscope slides, which contained a small, platinum heating coil (~5 mm long, 3 mm internal diameter) at its approximate center. The heating coil holds the glass sample (typically from 60 to 280 mg) and a Platinum-13% Rhodium thermocouple for temperature measurements, see ref. [13] for further details.

As mentioned in the introduction, this part of the paper describes the analysis and characterization of the melts that were splattered and solidified on the bottom plate of the experimental glass box during high gravity (8 to 10-g) deceleration of the drop capsule. To investigate the effect of substrate material on the solidification and crystallization of the melts, plates of alumina, glass, copper, gold and platinum were used for the bottom plate of the glass box. The other parameter whose effect on the melt solidification and crystallization was investigated was the melt temperature, which was controlled by varying the current through the heating coil. The same experiment ID as was used in ref. [13] was used also in the present paper, an example of which is "NT_4-5Al". The letters and numbers preceeding the hypheu indicate the type of glass, which in this case is $Na_2O \cdot 4TeO_2$. The number after the hyphen denotes the experiment number for this glass (in this case, 5th experiment for the NT_4 glass), and the letters following this number denotes the substrate material, which is "alumina" in this case. The substrate materials glass, alumina, copper, gold and platinum are abbreviated as Gl, Al, Cu, Au and Pt, respectively. The surface of the substrate plates, on which the melts splattered, was polished and washed with acetone to make them smooth and free from dirt.

The splatters from the drop shaft experiments were observed by optical and scanning electron microscopy (SEM), and chemically analyzed on both surfaces by energy dispersive x-ray analysis (EDS). The glass transition temperature (T_g), crystallization temperature (T_p), and the activation energy for crystallization (E) for the splatters were measured by differential scanning calorimetry (TA Instrument DSC 2010) at heating rates of 5, 10, 20, 30 and 40°C/min using covered aluminum pan and a typical sample mass of 10 mg. A high purity (99.99%) α-Al_2O_3 powder provided by the instrument supplier, was used as a reference standard. The following thermoanalytical model due to Kissinger [14] was used to determine E,

$$\ln\left(T_p^2/\phi\right) \propto E/(RT_p) \tag{1}$$

where, ϕ is the DSC heating rate, and R is the gas constant.

The heat capacity (C_p) in the glass transition region for the samples was measured (TA-DSC 2010) at 10°C/min using a sample mass of about 20 mg and α-Al_2O_3 as the calibration standard. The sample was placed in an aluminum pan (TA 900786.901) with a lid (TA 900779.901) on top of the sample and sealed using a crimping die for the heat capacity measurements

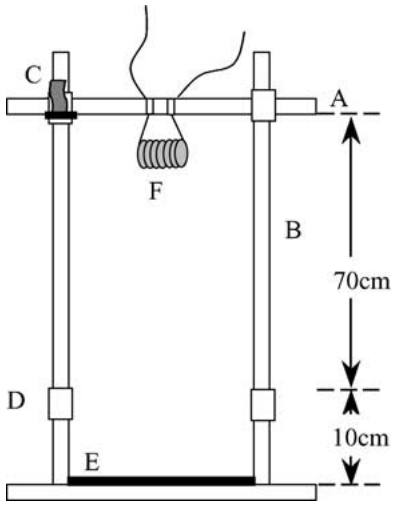

Figure 1 Schematic for preparing splatters in ground experiments. A: Fixture, B: Steel post, C: Release lever mechanism, D: Stoppers, E: Substrate plate, F: Heating coil holding the melt.

in DSC. All the DSC measurements (for T_g, T_p, E and C_p) were conducted in a flowing (30 cm^3/min) nitrogen gas.

The Fourier Transform Infrared (FTIR) spectra for the samples were measured from 1000 to 400 cm^{-1} using the standard KBr technique. The spectra for pure KBr was measured first to make the necessary background correction.

Splatters similar to those obtained from the drop shaft experiments were prepared at 1-g (ground) for comparative property evaluation. In ground experiments, about 150 mg of the glass was fused to a platinum heating coil that was identical to those used in the drop shaft experiments, see the schematic in Fig. 1 for the ground-based experimental arrangement.

The heating coil (F) holding the glass was mounted in a fixture (A) that slides vertically along two steel posts (B). The fixture was initially held at a height of about 120 cm from the bottom by a release lever mechanism (C). The glass was melted for about 25 s using the same maximum current (through the coil) as was used in the drop shaft experiment. The fixture holding the melt in the coil was then released by operating the lever, *C*, and made to fall until it hit the two stops (D) that were rigidly clamped to the steel posts, B. The melt detached from the heating coil when the fixture, A, hit the stops, D, and splattered onto a substrate plate, E, positioned just below the heating coil. The height of the stops were adjusted so that the distance between the substrate plate (E) and the coil was about 4 cm when the fixture, A, was at rest on D. This 4 cm distance between the heating coil and the substrate plate is the same as what was maintained in the drop shaft experiments.

3. Results and discussion

A total of ten experiments, five each for the NT_8 and NT_4 glasses, were conducted in the JAMIC drop shaft. One experiment with the NT_8 glass (NT_8-1Gl) failed due to a problem with the heating coil. The experimental parameters, namely, the voltage and current through the heating coil, the melt temperature, and the gravity value as a function of time in low gravity for each experiment are given in ref. [13], and will not be repeated here. The gravity level (Z-direction, vertical to the axis of the heating coil) during free-fall of the capsule was highly reproducible in different experiments, and was $<20 \times 10^{-4}$ g ($\pm 5 \times 10^{-4}$ g) during the 10 s of low gravity and 8 to 10-g during capsule deceleration. The maximum melt temperature as measured by a thermocouple imbedded in the melt varied from ~770 to 1090°C in different experiments, and appeared to have no effect on the properties of the solidified melts. The melt temperature for these experiments, therefore, will not be separately shown, but can be found in ref. [13].

3.1. Splatters

The melt remaining in the coil after evaporation became detached from the heating coil during capsule deceleration (braking) and was splattered on the substrate (bottom) plate, producing several splatters of different size. The number of splatters in different experiments varied from 2 to 6, with diameters from 1 to 8 mm and thickness from 0.5 to 2 mm. The larger splatters had a smaller thickness. Analysis by SEM and optical microscopy showed that all the NT_8 splatters obtained from different drop experiments were transparent glass and no crystals were found either on the surface or in the interior. Similar transparent, glassy splatters were also obtained from ground experiments (1-g) for the NT_8 melts.

Unlike the splatters from experiments with the NT_8 melts, the splatters for the NT_4 melts partially crystallized in all the 5 drop-experiments conducted at JAMIC. The typical splatters obtained from the drop shaft experiments and the morphology of the crystals on the surface of these splatters are shown in Figs 2 and 3, respectively. The splatters for the NT_4 melts in our previous drop experiments [15, 16] at JAMIC also crystallized, but those results were not given a high level of confidence at that time, since this NT_4 melt is an excellent glass former and difficult to crystallize at 1-g. The present results not only confirmed our previous results, but established that an NT_4 glass would always crystallize (at least, partially) when melted and quenched in the drop shaft environment. As analyzed by EDAX, the composition of the crystals is essentially the same as that of the starting NT_4 glass.

The concentration of crystals on the bottom surface of the splatters (surface in contact with the substrate plate) is generally higher than that of the crystals on the top surface (surface in contact with air/vapor), compare (a) with (b) or (c) with (d) in Fig. 2. The reason for a higher concentration of crystals on the bottom surface than on the top surface is not quite clear, but may be that the substrate material provided a larger number of heterogeneous nucleation centers, which caused the bottom surface of the splatter to crystallize more extensively than the top surface. However, neither the size nor the general morphology of the crystals on the top surface is very much different from that of the crystals on the bottom surface. The size of the crystals ranged

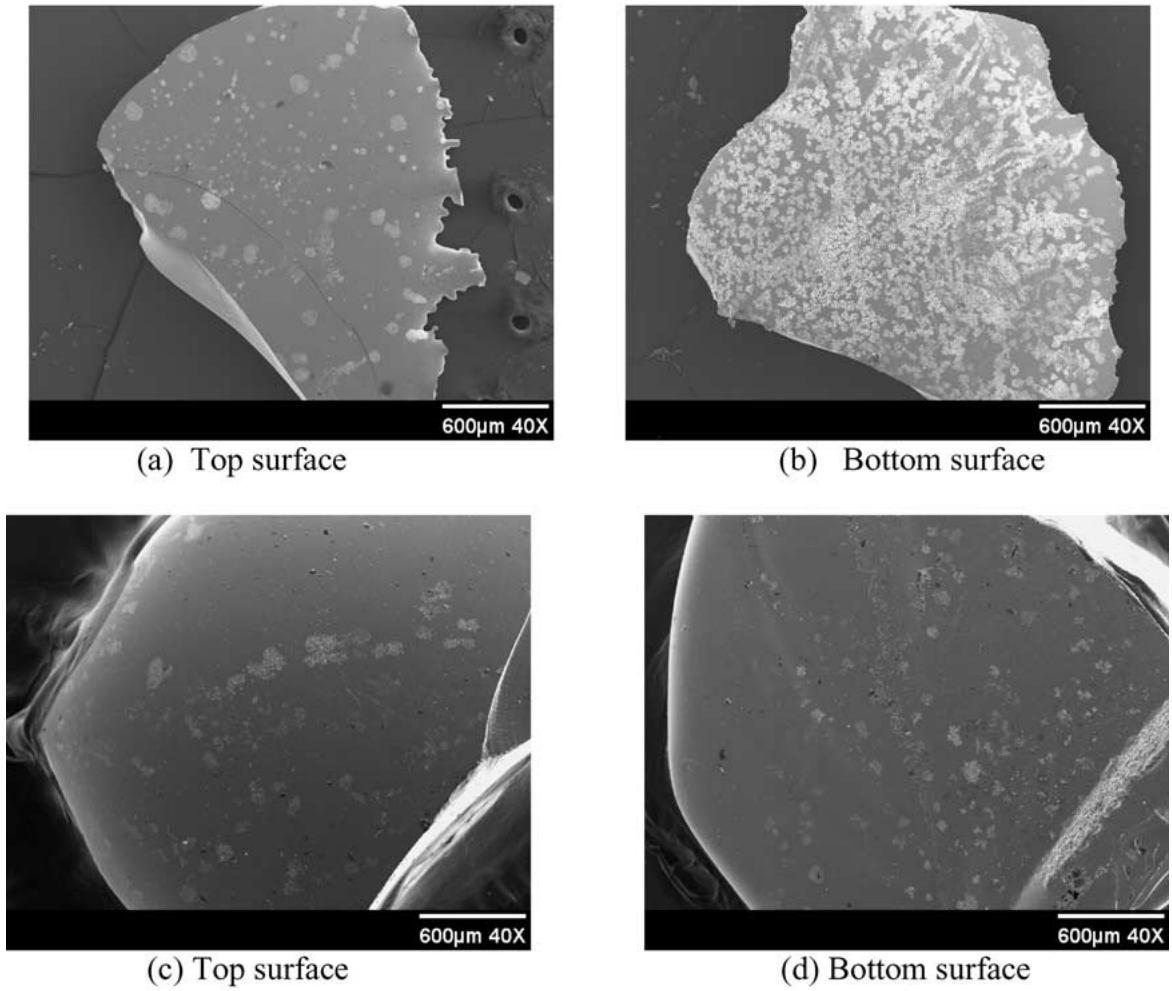

Figure 2 Top and bottom surface of the splatters from JAMIC drop shaft experiments (a, b) NT_4-3Gl and (c, d) NT_4-1Cu. The crystals (white regions or spots) are clearly visible on the surface of the splatters.

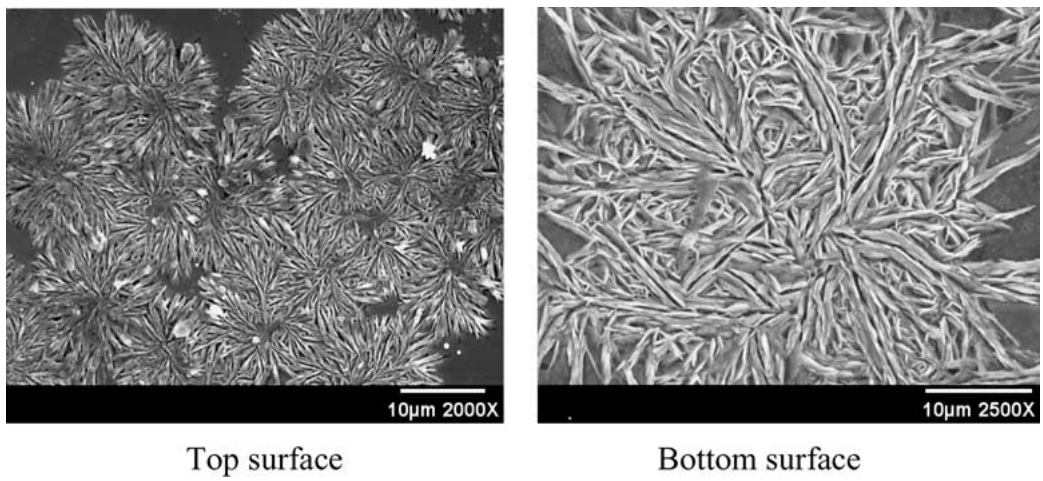

Figure 3 Typical morphology of the crystals on the top or bottom surface of the NT_4 splatters (Expt. NT_4-3Gl) from JAMIC drop shaft experiments.

typically between 10 and 100 μm, and the size of the majority (60 to 70%) of crystals was between 40 and 60 μm.

The concentration of crystals on either the top or bottom surface of the splatters varied with the substrate material on which the melt splattered, compare (a) with (c) or (b) with (d) in Fig. 2. The substrate material for the splatter in Fig. 2a and b was a glass and that for the splatter in Fig. 2c and d was copper. Clearly, the concentration of crystals on a splatter on the glass substrate is higher than that on a splatter on the copper substrate. It is believed that the melt on a glass substrate cooled at a slower rate than the melt on the copper substrate, which caused the splatter on the glass substrate to crystallize more heavily than the splatter on the copper substrate.

A term "heat diffusivity, δ" of a material, which is different from thermal diffusivity, h $(=K/d \cdot C_{\mathrm{p}})$ and which measures the ability of the material to extract and

TABLE I Heat diffusivity of the substrate materials

Substrate materials	Density, d (g/cm^3)	Heat conductivity, K (W/cmK)	Heat capacity, C_p (J/gK)	Heat diffusivity (δ)
Copper	8.92	4.01	0.385	13.77
Au	19.31	3.17	0.129	7.90
Pt	21.45	0.72	0.133	2.04
Al_2O_3	3.96	0.35	0.780	1.08
Glass	2.30	0.01	0.840	0.02

Note: Heat diffusivity, $\delta = d \times K \times C_p$.

dissipate heat from a melt cast on it, is defined as [17] $\delta = d \times K \times C_p$, where d is the density, K is the thermal conductivity, and C_p is the heat capacity of the material. A material with a higher value of δ should extract and dissipate heat at a faster rate from a melt dropped on it, thereby, causing the melt to cool at a faster rate. The heat diffusivity of the substrate materials used in the present drop experiments was calculated from their known values of d, K, and C_p and is shown in Table I. Table I shows that δ for the materials decreases in the order $\delta_{Cu} > \delta_{Au} > \delta_{Pt} > \delta_{Alumina} > \delta_{Glass}$. The cooling rate experienced by a melt dropped on these substrates will also decrease in the same order. Therefore, the crystal density X of the splatters is expected to decrease in the order $X_{Glass} > X_{Alumina} > X_{Pt} > X_{Au} > X_{Cu}$, which is consistent with the present results.

The different "wetting" of the material by the melt may also be a reason for the observed difference in crystal density in different splatters. Oxide materials such as glass or alumina are, generally, wetted more (smaller contact angle) by a melt or liquid than metals such as copper, gold, or platinum. This causes the energy barrier for nucleation in a melt on an oxide substrate to decrease, thereby, causing its overall tendency for crystallization to increase compared to that of the same melt on a metal substrate. However, none of the NT_4 splatters crystallized in ground experiments when splattered on different substrates. So, the effect of substrate materials on crystallization of the melt could not be investigated at 1-g.

While the present experiments confirm that an NT_4 glass will crystallize when melted and quenched in a drop shaft environment, the exact reason for crystallization of this melt is still largely unknown. Small splatters (100 to 150 mg) of this glass prepared at 1-g did not crystallize when splattered on any of the substrates used in the drop shaft experiments, namely, glass, alumina, gold, platinum, and copper. Even, crystal-free glass bars of 1 cm × 1 cm × 5 cm are easily obtained by normal casting of this NT_4 melt at 1-g onto steel molds. Why these very small pieces (30 to 60 mg, Figs 2 and 3) of rapidly quenched NT_4 melt crystallized in the drop shaft experiments remains an interesting problem.

One possible reason for the observed crystallization of the NT_4 splatters may be that these melts were solidified not in low-g, but at a high-g (8 to 10 g) after they detached from the heating coil during capsule deceleration. As mentioned earlier, results from numerous experiments conducted to date in space show [4–11] that the glass forming tendency for melts is enhanced in low gravity compared to identical melts on earth (1-g), or stated conversely, the crystallization tendency for a melt is enhanced with increasing gravity. Thus, the results for the crystallization of the NT_4 melts in the drop shaft experiments are consistent with the reported results on glass formation for many oxide, chalcogenide and metallic melts in space.

Another possible reason for a higher crystallization tendency for the NT4 melt maybe that the NT_4 glass is more readily attacked by moisture than the NT_8 glass. The measured dissolution rate(DR) in water at room temperature for the NT_4 glass is $\sim 8.1 \times 10^{-5}$ g · cm^{-2} min^{-1}, which is about 4 times larger than that for the NT_8 glass($\sim 2.3 \times 10^{-5}$ g · cm^{-2} min^{-1}). This means that the aqueous chemical durability of the NT_4 glass is ~4 times smaller than that for the NT_8 glass, which makes it more susceptible to crystallization than the NT_8 glass. In any case, the glass forming ability of the NT_8 melt is considered higher than that of the NT_4 melt, since the NT_8 melt did not crystallize in any of the drop shaft experiments, whereas, the NT_4 melt partially crystallized in all the drop shaft experiments.

3.2. Thermal properties

3.2.1. Glass transition, crystallization and melting temperatures

The DSC patterns for the NT_8 splatters prepared at 1-g on different substrates were essentially the same and indistinguishable from each other, but they are considerably different for the NT_8 and NT_4 splatters. Typical DSC patterns for the 1-g NT_8 and NT_4 splatters on a glass substrate are shown in Fig. 4. Compared to that for the NT_4 glass, the DSC pattern for the NT_8 glass contains two additional peaks, an endothermic peak (T_{m1}) at ~375°C and one exothermic peak (T_{p2}) at about 435°C. The first small endothermic peak in the curves in Fig. 4 corresponds to the glass transition, T_g. The glass transition temperature, T_g, as determined by the technique shown at the inset, is 274 and 256 (±2)°C for the NT_8 and NT_4 glasses, respectively.

Although, the T_g for the NT_8 glass is about 18°C higher than that for the NT_4 glass, the temperature of

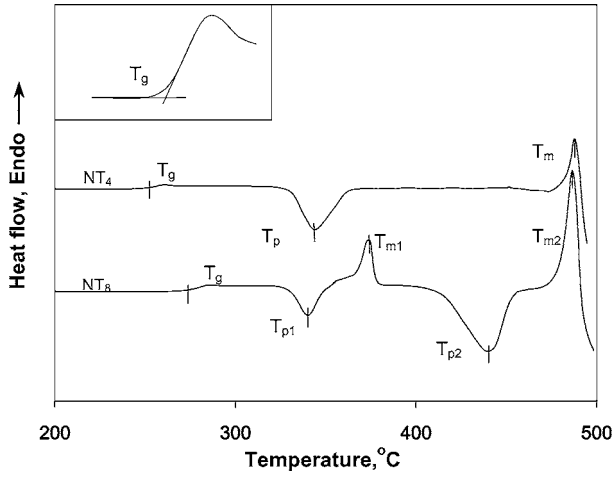

Figure 4 DSC curves at 10°C/min for NT_4 and NT_8 splatters on a glass substrate from ground experiments.

TABLE II Thermal analysis (DSC) results at heating rate of 10°C/min for the NT_8 and NT_4 splatters from the ground and JAMIC drop shaft experiments

Exp. ID	T_g (±2) (°C)	T_{p1} (for NT_8) or T_p (for NT_4) (±2) (°C)	T_{p2} (±2) (°C)	T_{m1} (±2) (°C)	T_{m2} (for NT_8) or T_m (for NT_4) (±2) (°C)	ΔH for T_{p1} (NT_8) or T_p (NT_4) peaks (±4) (J/g)	ΔH for T_{p2} peak (±4) (J/g)	Activation energy, E(±10) (kJ/mol)
Ground (NT_8-Gl)	274	341	435	374	475	36	138	252
NT_8-2Gl	275	336	432	375	476	38	137	278
NT_8-3Cu	275	330	432	377	475	38	138	280
NT_8-4Gl	274	338	433	374	474	38	124	289
NT_8-5Al	275	337	432	375	476	38	130	285
Ground (NT_4-Gl)	254	345	–	–	475	71	–	213
NT_4-1Cu	253	333	–	–	477	74	–	251
NT_4-2Pt	254	336	–	–	476	77	–	247
NT_4-4Au	253	336	–	–	476	80	–	243
NT_4-5Al	253	340	–	–	477	81	–	240

See Fig. 4 for a description of the characteristic temperatures (T_g, T_p, T_{p1}, T_{p1}, T_{p2}, T_m, T_{m1}, T_{m2}). ΔH is the heat of crystallization. The activation energy, E, for the NT_8 glass was determined from the analysis of its first crystallization peak (T_{p1}).

the first exothermic peak, T_{p1} (341 ± 2°C), for the NT_8 glass is very close to that of the exothermic peak, T_p (345 ± 2°C), for the NT_4 glass. Likewise, the final melting or liquidus temperature (endothermic peak, T_{m2} for NT_8 and T_m for NT_4) is essentially the same for these two glasses, about 475°C.

The DSC exothermic peak, T_p, for the NT_4 glass was identified by XRD to be due to the crystallization of NT_4 crystals only. The crystalline phase corresponding to the exothermic peak, T_{p1}, for the NT_8 glass could not be identified. It is believed that a crystalline phase whose composition is close or same as NT_8 exists in this system, and the first exothermic DSC peak for the NT_8 glass (T_{p1} in Fig. 4) occurs due to the formation of these crystals. The possible existence of an NT_8 compound in the sodium-tellurite system, which has not been reported up to this time, is discussed elsewhere [18].

The second DSC exothermic peak, T_{p2}, for the NT_8 glass was identified to be to simultaneous crystallization of TeO_2 and NT_4, which is in accordance with the existing phase diagram for the Na_2O – TeO_2 system [19].

The reason for the appearance of the endothermic peak, T_{m1}, for this glass is not known for certain, but may be due to some reaction and dissolution of the NT_8 crystals in the glass matrix.

The DSC patterns for the NT_8 or NT_4 splatters from the drop shaft experiments are nearly identical to that of their 1-g counterparts, see Figs 5 and 6 for the NT_8 and NT_4 glasses, respectively. The glass transition, crystallization, and melting temperatures, and the heat of crystallization (ΔH) determined from the curves in Figs 5 and 6 are shown in Table II for each of the drop shaft and 1-g splatters. Figs 5 and 6, and Table II show that except for a small difference in the crystallization temperature (first crystallization temperature for the NT_8 glass), all other characteristic temperatures for the drop shaft splatters are nearly the same as those for the 1-g splatters for a same glass composition. Like the values for the characteristic temperatures, the heat of crystallization, ΔH, for the drop shaft and 1-g splatters does not differ, also. In other words, the

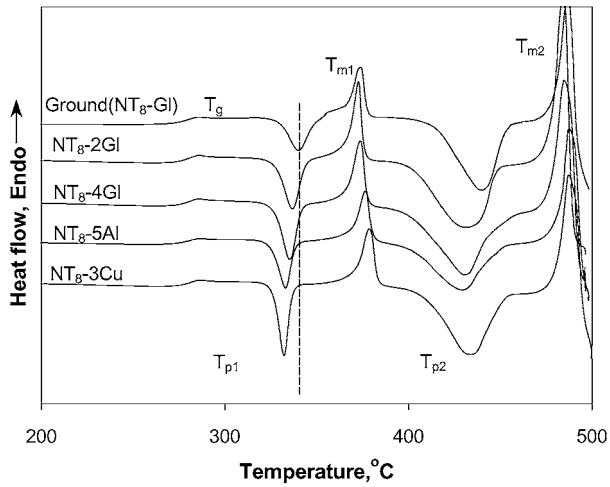

Figure 5 DSC curves at 10°C/min of NT_8 splatters from JAMIC drop shaft and ground experiments. All curves except the one marked as ground are for drop shaft samples.

thermal analysis results for either NT_8 or NT_4 splatters from different drop experiments are the same, consistent and reproducible, and are in close agreement with those for similar splatters from ground experiments. The effect of gravity as experienced in the drop shaft environment at JAMIC on the thermal properties of NT_8 and NT_4 glasses is, therefore, considered negligible.

It is interesting to note that the first crystallization temperature for all the NT_8 drop shaft splatters is consistently 3 to 11°C lower than that of the 1-g splatter, see Fig 5 and Table II. Similar decrease (5 to 12°C) in the crystallization temperature for the drop shaft splatters compared to that for the 1-g splatters is also observed for the NT_4 glass, Fig 6 and Table II. Although the difference is small, a consistent and reproducible decrease in the crystallization temperature for the drop shaft splatters might indicate that they are less resistant to crystallization than their 1-g counterparts. It may be recalled that the splatters in the drop shaft experiments were formed through solidification of melts at 8 to 10-g, which leads to suggest that a melt becomes less resistant

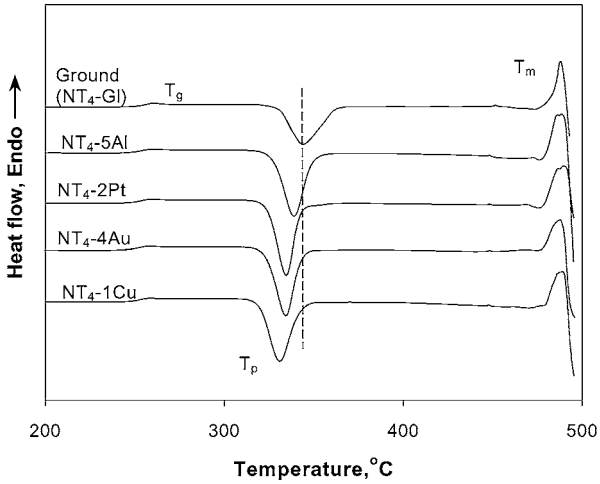

Figure 6 DSC curves at 10°C/min of NT_8 splatters from JAMIC drop shaft and ground experiments. All curves except the one marked as ground are for drop shaft samples.

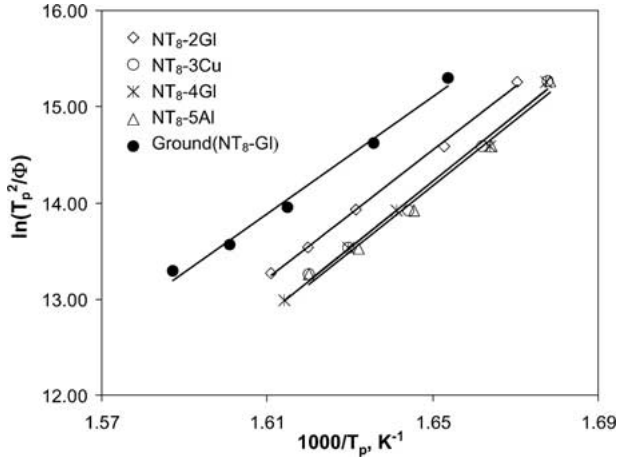

Figure 7 Plots of $\ln(T_p^2/\Phi)$ vs $1/T_p$ (Equation 1) for the NT_8 splatters from JAMIC drop shaft and ground experiment. All curves except the one marked as ground (solid circle) are for drop shaft samples.

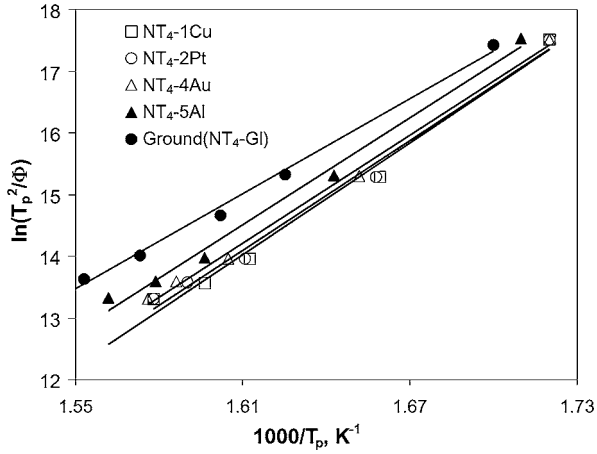

Figure 8 Plots of $\ln(T_p^2/\Phi)$ vs $1/T_p$ for the NT_4 splatters from JAMIC drop shaft and ground experiments. All curves except the one marked as ground (solid circle) are for drop shaft samples.

to crystallization with increasing gravity. This is consistent with the reported results [4–11] from numerous experiments conducted on glass forming melts in space.

For any particular composition, there is practically no difference in the heat of crystallization, ΔH, (Table II) for the drop shaft and 1-g splatters. The average ΔH for the NT_4 splatters, ~76 (±5) J/g, is twice the average ΔH, ~38 J/g, for the first crystallization peak of the NT_8 splatters. This result might suggest that the NT_4 crystals are more stable than the NT_8 crystals, which are believed to form as the first crystallization product in the NT_8 glass. It has been demonstrated in ref [18] that this NT_8 crystalline phase is not a stable, but metastable phase. A high average ΔH value, ~134 (±8) J/g, for the second crystallization peak of the NT_8 splatters is consistent with the fact that this peak occurs due to the crystallization of two most stable crystals in this sodium-telurite system, namely, NT_4 and TeO_2.

3.2.2. Activation energy for crystallization

A plot of ln (T_p^2/ϕ) vs $1/T_p$ should be a straight line according to Equation 1, and the activation energy for crystallization, E, can be determined from the slope of this straight line. Typical ln (T_p^2/ϕ) vs $1/T_p$ plots for the NT_8 and NT_4 drop shaft and 1-g splatters are shown in Figs 7 and 8, respectively. The values of E calculated from the slope of the straight lines in Figs 7 and 8 are given in column 9 of Table II. Table II shows that the values of E for all the drop shaft splatters for any given composition are very close, but they are clearly higher for NT_8 than that for NT_4 composition (283 ± 5 kJ/mol for the NT_8 and 245 ± 5 kJ/mol for the NT_4 compositions). The E-value for the 1-g splatters is also higher for NT_8 (252 kJ/mol) compared to that for NT_4 (213 kJ/mol). The average value of E for the drop shaft splatters is 12 to 15% higher than that of the 1-g splatters for both compositions.

A higher average E-value for the NT_8 than that for the NT_4 drop shaft or 1-g splatters suggests that the NT_8 melt is more resistant to crystallization or is a better glass former than NT_4. This has been qualitatively observed also by comparing the crystallinity on the as-received NT_8 and NT_4 splatters from drop shaft experiments, see Section 1 above for splatters. Similar comparison of E-values suggests that the drop shaft splatters should be more resistant to crystallization than the 1-g splatters for any composition, but this is what has not been reflected in the DSC patterns, see Figs 5 and 6. The DSC results in Figs 5 and 6 show that the drop shaft splatters crystallize at lower temperatures for both compositions, suggesting the drop shaft splatters are less resistant to crystallization than their 1-g counterparts.

A conclusion somewhat opposite to what has been made above from comparison of E-values is arrived at when the glass forming parameter, $K_{gl} = (T_p - T_g)/(T_m - T_p)$, for these splatters is compared. The average values of K_{gl} for different splatters calculated from their characteristic temperatures (T_g, T_p, and T_m) in DSC curves (Figs 5 and 6, Table II) are given in Table III. The results in Table III show that the values of K_{gl} for both the drop shaft and 1-g splatters for NT_4 composition are larger than the K_{gl} values for the corresponding NT_8 splatters. Also, the K_{gl} values for the

TABLE III Average glass forming parameter, K_{gl}, for the NT_8 and NT_4 drop shaft and 1-g splatters

Composition of splatters	Gravity condition	$K_{gl} = (T_p - T_g)/(T_m - T_p)$
$Na_2O \cdot 8TeO_2$ (NT_8)	1-g	0.49 ± 0.02
	Drop shaft	0.42 ± 0.04
$Na_2O \cdot 4TeO_2$ (NT_4)	1-g	0.68 ± 0.02
	Drop shaft	0.58 ± 0.04

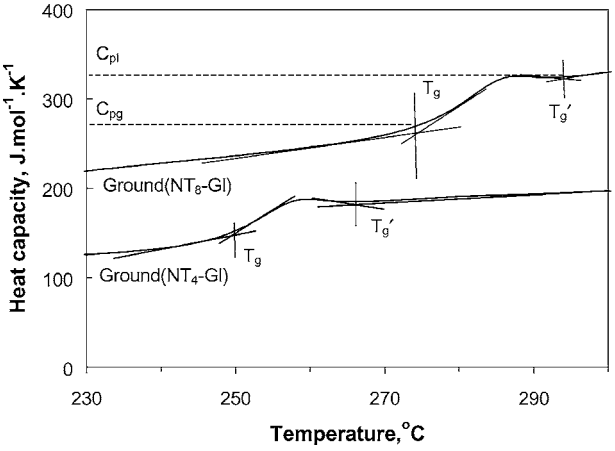

Figure 9 Typical heat capacity curves at 10°C/min for the NT_8 and NT_4 splatters on a glass substrate from ground experiments.

drop shaft splatters are smaller than that of the 1-g splatters for both compositions. These results suggest that the NT_8 glass is less resistant to crystallization than the NT_4, and the drop shaft splatters are also less resistant to crystallization than their 1-g counterparts for both compositions. Clearly, this conclusion is opposite to what has been observed above from a comparison of the E-values for these splatters. Why the analysis of K_{gl} and E values for these splatters yield opposite results is not clearly understood at this time, and further work seems necessary to clarify this point.

3.2.3. Heat capacity

The heat capacity (C_p) in the glass transition region obtained at a heating rate of 10°C/min for the 1-g NT_8 and NT_4 splatters is shown in Fig 9. C_p increases fairly rapidly during transition from the glass to liquid state, producing an S-shaped curve. This overall S-shaped C_p vs temperature curve in the glass transition region is typical of most glass and polymeric materials. The method of determining the lower and upper temperature end of the glass transition region, marked T_g and T_g', respectively, is also shown on the curves. The lower temperature end of the glass transition region, T_g, is generally taken as the glass transition temperature. The value of C_p at T_g is referred to as the heat capacity of the glass, C_{pg}, and that at T_g' is referred to as the heat capacity of the liquid state, C_{pl}.

The C_p vs temperature curves for the drop shaft and 1-g splatters for the same composition are nearly indistinguishable from each other. These are shown in Figs 10 and 11 for the NT_8 and NT_4 splatters respectively, where the curves are intentionally displaced in the vertical direction for clarity. The values of T_g, T_g', C_{pg}, C_{pl}, width of glass transition (T_g'–T_g), and the ratio C_{pl}/C_{pg} determined from these curves and given in Table IV, show that they are not different for the drop shaft and 1-g splatters for a given composition. The values of T_g determined from the C_p vs temperature curves are the same, within ±1°C, as those determined from the crystallization curves in Figs 4–6, and are in excellent agreement with the T_g values for the lithium-tellurite glasses [20] of comparable compositions.

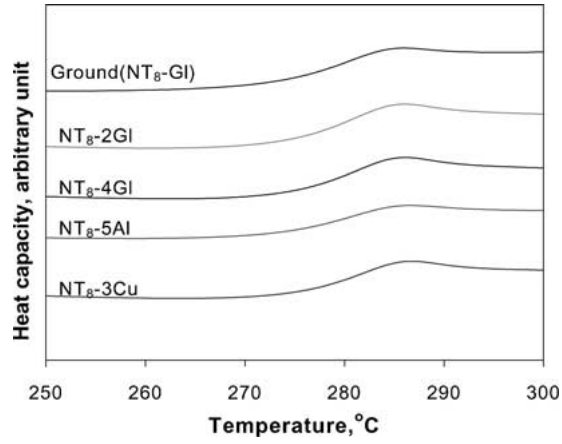

Figure 10 Heat capacity curves at 10°C/min for the NT_8 splatters from ground and JAMIC drop shaft experiments. All curves except the one marked as ground are for drop shaft samples. The curves are intentionally displaced in the vertical direction for clarity.

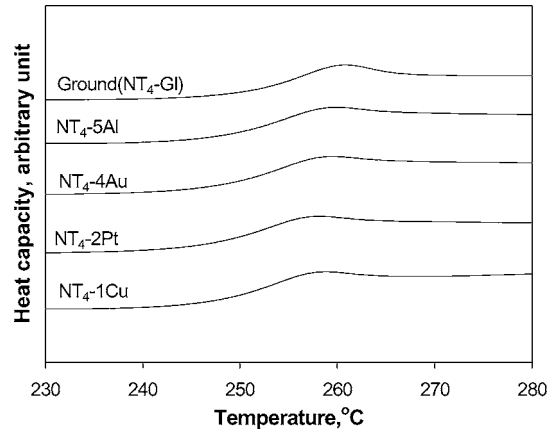

Figure 11 Heat capacity curves at 10°C/min for the NT_8 splatters from ground and JAMIC drop shaft experiments. All curves except the one marked as ground are for drop shaft samples. The curves are intentionally displaced in the vertical direction for clarity.

The average value of heat capacity at T_g for the NT_8 splatters (C_{pg}), 267 ± 8 Jmol^{-1} K^{-1}, is much higher than that for the NT_4 splatters, 142 ± 6 Jmol^{-1} K^{-1}. The glass transition region, $T_g' - T_g$, is also a little wider for the NT_8 splatters, 15 to 16°C compared to 12 to 13°C for the NT_4 splatters. The reasons for a wider glass transition region and higher value of C_{pg} for the NT_8 splatters compared to those for the NT_4 splatters are not clearly understood, and further investigations are necessary. When expressed in unit of cal · g^{-1} · K^{-1}, the average values of C_{pg} for these glasses (0.43 cal · g^{-1} · K^{-1} for NT_8 and 0.24 cal · g^{-1} · K^{-1} for NT_4) are found to be within the

TABLE IV Heat capacity in the glass transition region for the NT_8 and NT_4 drop shaft and 1-g splatters

Exp.ID	T_g(±2) (°C)	Heat capacity of glass, C_{pg}(±5) (J/mol · K)	T_g'(±2) (°C)	Heat capacity of supercooled liquid C_{pl}(±5) (J/mol · K)	Glass transition width (T_g'-T_g) (°C)	C_{pl}/C_{pg} (±0.04)
Ground (NT_8-Gl)	274	262	289	312	15	1.19
NT_8-2Gl	275	268	290	320	15	1.19
NT_8-3Cu	275	271	291	319	16	1.18
NT_8-4Gl	274	265	290	320	16	1.21
NT_8-5Al	275	277	291	328	16	1.18
Ground (NT_4-Gl)	254	144	267	188	13	1.30
NT_4-1Cu	253	136	265	177	12	1.30
NT_4-2Pt	254	141	267	183	13	1.30
NT_4-4Au	253	140	265	185	12	1.32
NT_4-5Al	253	149	265	195	12	1.31

See Fig. 9 for a description of the parameters.

range of C_{pg} values for the conventional silicate, borate, and phosphate glasses (0.2 to 0.5 cal · g^{-1} · K^{-1}).

The average value for the ratio C_{pl}/C_{pg} for the NT_8 and NT_4 splatters is 1.30 and 1.16 (±0.02), respectively. According to Angell's strong/fragile liquid classification [21], a strong liquid such as SiO_2 or GeO_2, shows a small change in heat capacity at T_g ($C_{pl}/C_{pg} \sim 1.1$). A fragile liquid is characterized as one having a large change (60 to 80%) in heat capacity at T_g. For a heavy metal fluoride (ZBLAN) [22] or a $40Fe_2O_3 - 60P_2O_5$, mol%, glass [23], which are considered typical fragile liquids, the value of C_{pl}/C_{pg} is about 1.6. Based on this classification, the NT_8 and NT_4 liquids can be characterized as moderately strong, and NT_8 appears a little stronger than NT_4.

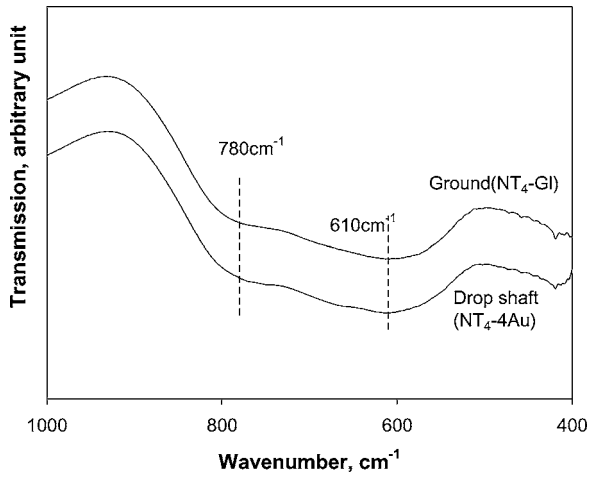

Figure 13 Typical IR spectra for the NT_4 splatters from the ground and JAMIC drop shaft experiments.

3.3. IR spectra

The IR vibrational bands for the tellurite glasses mostly occur in the 400 to 1000 cm^{-1} wavenumber range, so the IR spectra for the splatters in the present investigation were also measured in this range. The general features of the IR spectra are similar for the NT_8 and NT_4 splatters, and indistinguishable for 1-g and drop shaft splatters. Examples of typical IR spectra are shown in Figs 12 and 13 for the NT_8 and NT_4 splatters, respectively. In each figure, the IR spectra for a splatter from one of the drop experiments have been compared with that for a 1-g splatter, and the curves are intentionally displaced in the vertical direction for clarity. As shown in Figs 12 and 13, there is practically no difference in the IR spectra for any of these splatters.

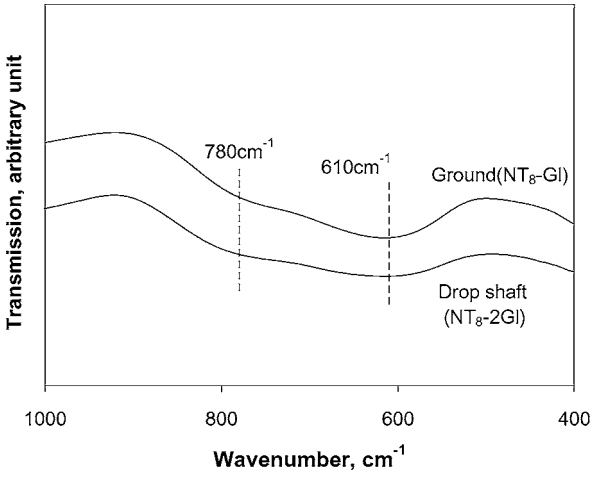

Figure 12 Typical IR spectra for the NT_8 splatters from the ground and JAMIC drop shaft experiments.

The general features of the IR spectra shown in Figs 12 and 13 are similar to those for the sodium-tellurite [24] and lithium-tellurite [24, 25] glasses reported by others. It has been demonstrated [24–26] that the structure of tellurite glasses is composed primarily of a three dimensional network of distorted [TeO_4] trigonal bipyramids (tbps), in which the tellurium atom is surrounded by two oxygen atoms at axial positions (O_{ax}), two oxygen atoms at equatorial positions (O_{eq}), and a lone pair of electrons at a third equatorial position. Addition of modifier oxides such as Na_2O or Li_2O breaks the Te-O-Te bonds and forms [TeO_3] trigonal pyramid (tp) with non-bridging oxygens. The absorption at 600–620 cm^{-1} is believed [24–27] to be due to the asymetrical stretching vibration of Te-O_{ax} bonds and that at 780–800 cm^{-1} is due to the symetrical stretching vibration of Te-O_{eq} bonds. The results from IR spectra could not reveal any difference between the network structure of 1-g and drop shaft splatters.

4. Conclusions

Re-melting and solidifying the melts of NT_8 and NT_4 glasses in the 10 s low gravity ($<10^{-3}$ g) drop shaft at JAMIC, produced transparent glass for the NT_8 composition, but produced a partially crystallized glass for the NT_4 composition. These results were reproducible in all five experiments conducted for each of the NT_8 and NT_4 compositions. Both compositions form good, transparent glass at normal gravity on earth. The partial crystallization of the NT_4 glass was attributed to an effect of high gravity (8 to 10 g) at which the melts were solidified. The drop shaft experiments indicate that the glass forming tendency for the NT_8 melt is better than the NT_4 melt.

The glass transition temperature, heat capacity, and IR spectra for the drop shaft splatters are essentially the same as those for the 1-g splatters of either NT_8 or NT_4 composition. These results suggest that the characteristics of these sodium-tellurite melts solidified under drop shaft conditions are not significantly different from the melts of the same composition solidified at 1-g.

A slightly lower crystallization temperature of the drop shaft splatters for both compositions compared to that of their 1-g counterparts, suggests that the melts solidified in the drop shaft maybe slightly less resistant to crystallization than the similar melts solidified at 1-g. A lower resistance to crystallization for the drop shaft melts is attributed to the effect of high gravity. However, it should be emphasized that the experimental conditions for the shorter ground experiments could be different from those of the relatively longer and higher velocity drop shaft experiments. For example, the rate of heat extraction from the splattered melts in the drop shaft may be different from that of the melts at 1-g. Thus, it is difficult to conclude definitely whether the observed difference between the crystallization temperatures for the drop shaft and 1-g splatters is due to an effect of high gravity or due to different experimental conditions existed in the drop shaft and 1-g experiments.

Acknowledgement

The work was partly supported by National Aeronautics and Space Administration (NASA), contract # NAG8-1465. The authors also greatly appreciate the help and cooperation of the following persons and organizations: Dr. Hajimu Wakabayashi of Nihon Yamamura Glass Co. (Japan), Dr. Hisao Azuma of Osaka Prefecture University (Japan), Japan Microgravity Center (JAMIC), Japan, and New Energy&Industrial Technology Development Organization (NEDO), Japan.

References

1. L. R. TESTARDI, *Adv. Ceramics (Materials Processing in Space)* **5** (1983) 25.
2. D. E. DAY and C. S.RAY, *Progress in Astronautics and Aeronautics* **108** (1986) 165.
3. J. C. LEGROS, A. SANFELD and M. VELARDE, in "Fluid Sciences and Materials Science in Space, CH.III" (European Space Agency, Springer-Verlag, 1987) p. 83.
4. C. BARTA, L. STOURAC, A. TRISKA, J. KOCKA and M. ZAVETOVA, *J. Non-Cryst. Solids* **35/36** (1980) 1239.
5. C. BARTA, J. TRNKA, A. TRISKA and M. FRUMAR, *Adv. Space Res.* **1**(5) (1981) 121.
6. G. T. PETROVSKII, V. V. RYUMIN and I. V. SEMESHKIN, *Steklo i Keramika* **1** (1983) 5.
7. J. ZARZYCKI, G. H. FRISCHAT and D. M. HERLACH, in "Fluid Sciences and Materials Science in Space, Ch. XVII" (European Space Agency, Springer-Verlag, 1987) p. 599.
8. C. S. RAY and D. E. DAY, *Mat. Res. Soc. Symp. Proc.* **87** (1987) 239.
9. G. H. FRISCHAT, *J. Non-Cryst. Solids* **183** (1995) 92.
10. D. S. TUCKER, G. L. WORKMAN and G. A. SMITH, *J. Mater. Res.* **12**(9) (1997) 2223 and references there in.
11. D. S. TUCKER, R. N. SCRIPA, B. WANG and J. M. RIGSBEE, in Proc. 18th Int. Cong. On Glass, San Francisco, July 1998 (available in CD Rom).
12. H. REISS, M. MIILLER, R. PASCOVA and I. GUTZOW, *J. Non-Cryst. Solides* **222**(1/2) (2001) 328.
13. D. ZHU, C. S. RAY, M. MAKIHARA, W. ZHOU and D. E. DAY, *J. Mater. Sci.* **37** (2002).
14. H. E. KISSINGER, *J. Res. Nat. Bur. Stand.* (U.S.) **57**(4) (1956) 217.
15. C. S. RAY, D. E. DAY, M. MAKIHARA and J. HAYAKAWA, -655 in Proceedings of 19th International Symposium on Space Technology and Science (ISTS), Tokyo, Japan, 1994 edited by M. Hinada (Hakushinsha Co., 1994) p. 651.
16. M. MAKIHARA, C. S. RAY and D. E. DAY, *Proce. SPIE* **3792** (1999) 209.
17. D. R. POIRIER and E. J. POIRIER, in "Heat Transfer Fundamentals of Metal Casting" (The Minerals, Metals & Materials Society (TMS) Publication, Warrendale, 1992) p. 41
18. D. ZHU, W. ZHOU and C. S. RAY, *J. Mat. Sci. Lett.* **20** (2001) 1961.
19. B. P. TROITSKII, A. K. YAKHKIND and N. S. MARTYSHCHENKO, *Izv. Akad. Nauk Sssr*, *Neorg. Mater.* **3**(4) (1967) 741.
20. S. K. LEE, M. TATSUMISAGO and T. MINAMI, *Phys. Chem. Glasses* **35**(6) (1994) 226.
21. C. A. ANGELL, *J. Non-Cryst. Solides* **131–133** (1991) 13.
22. C. T. MOYNIHAN, *J. Amer. Ceram. Soc.* **76**(5) (1993) 1081.
23. X. FANG, Ph. D Thesis, Ceramic Engineering Department, University of Missouri-Rolla (2000).
24. J. HEO, D. LAM, G. H. SIGEL JR., E. A. MENDOZA and D. HENSLEY, *J. Amer. Ceram. Soc.* **75**(2) (1992) 277.
25. T. YOKO, K. KAMIYA, H. YAMADA and K. TANAKA, *ibid.* **71**(2) (1988) C70.
26. Y. DIMITRIEV, V. DIMITROV and M. ARNAUDOV, *J. Mater. Sci.* **18** (1983) 1353.
27. T. UCHINO and T. YOKO, *J. Non-Cryst. Solids* **204** (1996) 243.

Received 19 September 2001
and accepted 18 April 2002